Miroslav Macka
Per Andersson
Paul R. Haddad

Department of Chemistry,
University of Tasmania, Hobart,
Tasmania, Australia

Linearity evaluation in absorbance detection: The use of light-emitting diodes for on-capillary detection in capillary electrophoresis

A model which takes into account both stray light and polychromatic light was used to predict and evaluate linearity in on-capillary detection in capillary electrophoresis (CE). According to the model the stray light is the major factor which determines linearity under typical CE operating conditions. By calculating theoretical absorbance *versus* concentration plots, the influence of different levels of stray light and polychromatic light on linearity is demonstrated. Experimentally, six light-emitting diodes (LEDs) in the range from 563 to 654 nm were examined as light sources for on-capillary detection in CE. Fitting theoretical curves to measured linearity plots enabled determination of the values of both effective path length and stray light for a particular detection system. The detector linearity for the four LEDs was compared to mercury and tungsten lamps used with interference filters. For potassium permanganate as the test compound, the linear range for a 563 nm LED was two times greater than that for a mercury lamp operated at 546 nm. The relatively poor linearity of the mercury lamp detector is explained by its high level of stray light. The noise of the LED563-based detector was the same as for the mercury lamp, whereas the other LEDs of higher light intensity gave approximately half the noise of the mercury lamp. The lowest noise level of 3×10^{-5} AU was obtained for the LED at 554 nm (determined at a detector time constant of 0.1 s).

1 Introduction

Light-emitting diodes (LEDs) have been utilised in various types of optical detectors (absorbance, fluorescence, refractive index), chiefly for applications in HPLC and flow-injection analysis (FIA) [1]. The use of LEDs for on-capillary detection in capillary electrophoresis (CE) has also been reported [2, 3]. A noise level of 1×10^{-5} AU for a 1 s integration time was achieved [2], but linearity effects were not reported. The attractive features of LEDs as light sources are their low cost, small size, long lifetimes [4], good intensity and stability resulting in low noise, and the possibility of direct electronic modulation of the light intensity [1, 4]. On the other hand, the disadvantages of LEDs include low light intensities for some varieties and the lack of commercially available LEDs for the UV region. A further important characteristic of LEDs is that the emission bandwidth (EBW) measured at half of the maximum emission intensity is 15–70 nm; they therefore provide moderately polychromatic light, which may result in poor detector linearity [5, 6].

Although this main disadvantage of LEDs is obvious, information on the response linearity of LED-based absorbance detectors is scarce. Good linearity was reported by Dasgupta *et al.* [1] for an absorbance detector using a 605 nm (31 nm EBW) LED and a 6 mm optical path length with alkaline bromothymol blue as the test compound. On the other hand, Hauser *et al.* [7, 8] used a number of routine analytical photometric methods to compare calibration graphs obtained with several LEDs used with a 10 mm path length flow-through photometer to those obtained on a conventional photometer. In most cases the comparison showed nonlinearity for the LED-based photometer, caused by the polychromatic light of the LEDs [7, 8], but the observed calibration curves were in good agreement with theoretical calculations based on numerical integration of the Beer-Lambert law over the entire LED emission spectrum and analyte absorption spectrum [8]. These conclusions regarding linearity of an LED-based photometer are applicable to path lengths in the mm range and may not be valid for on-capillary absorbance detection in CE where much lower absorbances are usually measured and high levels of stray light are present. For on-capillary absorbance detection in CE, the relative influences on linearity of stray light and polychromaticity have not been compared. The linearity of on-capillary detectors has been previously investigated only for monochromatic light [9–13]. The stray light, as an important parameter of an optical setup, is usually determined by measuring the transmittance of a totally absorbing solution in the cell [6, 9, 10]. However, this relatively simple procedure does not give any information on the value of the effective path length, another important parameter characterising the optical setup [6, 13].

There are several methods to investigate linearity. The American Society for Testing and Materials (ASTM) recommends a "static" linearity test for evaluation of absorption HPLC detectors [14], based on flushing the detector directly with calibration solutions of different concentrations of a test compound. This procedure elimi-

Correspondence: Prof. Paul R. Haddad, Chemistry Department, University of Tasmania, GPO Box 252C, Hobart, TAS 7001, Australia (Tel: +61-02-202179 (uni); Fax: +61-02-202858 (uni); E-mail: Paul.Haddad@chem.utas.edu.au)

Nonstandard abbreviations: ABW, absorption band width; **ASTM,** American Society for Testing and Materials; **BGE,** background electrolyte; **EBW,** emission band width; **LED,** light-emitting diode

Keywords: Capillary electrophoresis / Light-emitting diodes / On-capillary absorbance detection / Linearity

0173-0835/96/1212-1898 $10.00+.25/0

nates the influence of other components of the instrument and is also generally accepted as a valid linearity test for on-capillary detection in CE [9, 12, 13]. To evaluate the linearity data, several different approaches may be used. The most common method involves determining the correlation coefficient for all or part of a plot of absorbance *versus* concentration. However, it has been shown [15] that the correlation coefficient may not be sufficiently sensitive to nonlinearity, leading to an erroneous determination of the linear range. Another approach, the so-called Fowlis-Scott nonlinear function, has been used to test linearity of chromatographic detectors over a wide range of concentrations [16] and gives a response index which is ideally unity but acceptable linearity is indicated by values in the range of 0.98–1.02. However, this method is suitable only for calibration plots which exhibit the same curvature throughout the whole concentration range [15] and this is not the case when stray light exerts a major influence. Finally, the currently recommended procedure for evaluation of linearity data is the so-called linearity plot [15, 17, 18] which indicates minute changes in linearity and consequently gives more reliable information than other methods.

In this paper, the approach taken in the evaluation of linearity of LED-based on-capillary detectors in CE was based on the ASTM linearity test to acquire the data and then on the use of linearity plots to evaluate these data. Further, modelling of the experimental data has been used to characterise the optical configuration by determining two key parameters, namely the level of stray light and the effective path length through the capillary. Noise levels were also investigated and compared to those from alternative light sources.

2 Theory

2.1 Theoretical model

In the classical literature on UV/VIS molecular absorption spectrophotometry [5, 6], stray light is defined as light having wavelengths outside the range of the wavelength selector (*e.g.* monochromator) and which is not absorbed by the sample or not passed through the detector cell. Throughout this article, stray light is understood simply as light reaching the detector without passing the detector cell. Beer's law defines the absorbance A for an ideal case of a monochromatic beam and no stray light as:

$$A = \log \frac{P^0}{P} = \varepsilon_i \cdot b \cdot c \qquad (1)$$

where P^0 is the incident source radiant power, P is the emergent radiant power, ε is the molar absorptivity, c the concentration of the absorbing compound and b is the path length. After taking into account the stray light P_s and for a light beam composed of n different wavelengths $\lambda_1, \lambda_2 \ldots \lambda_i \ldots \lambda_n$, the absorbance is:

$$A = \log \frac{\sum P_i^0 + P_s}{\sum P_i + P_s} \qquad (2)$$

where P_i^0 is the incident source radiant power at the wavelength λ_i and P_i is the emergent radiant power at the same wavelength. Rewriting Eq. (1) for each wavelength and substituting into Eq. (2) gives:

$$A = \log \frac{\sum P_i^0 + P_s}{\sum P_i^0 \, 10^{-\varepsilon_i \cdot b \cdot c} + P_s} \qquad (3)$$

where ε_i is the molar absorptivity at wavelength λ_i. Equation (3) shows that the deviation from linearity of an absorbance *versus* concentration plot resulting from polychromatic light becomes more significant as the differences between the molar absorptivities at the different wavelengths increase, which will be governed by the absorption spectrum of the absorbing compound and the emission spectrum of the light source. The broadest range of molar absorptivities will be found when the emission maximum is positioned at the steepest slope of the absorption band, and for this case the theory predicts relative absorbance errors under 0.5% for a ratio of emission-to-absorption bandwidths of < 0.1, but this increases dramatically when the ratio exceeds 0.5 [6].

A limitation of the model described by Eq. (3) when applied to CE is that it does not account for refractive index changes causes by the solute itself or the variability of the path length resulting from the light passing at different places through the circuclar cross-section of the capillary. However, refractive index influences on the molar absorptivity are generally known to be insignificant at concentrations below 0.01 M [5], and the path length variability has been shown to be negligible for an incident beam of width 0.5 times the capillary diameter [6, 9, 11] and even for an incident beam width equal to the capillary diameter the linearity is still preserved at low absorbances [11]. In the present study a 75 μm capillary equipped with a 50 μm slit was used; path length variability was therefore neglected.

2.2 Modelling of linearity plots

It is useful to visualise Eq. (3) by showing the effects of several combinations of different levels of stray light with monochromatic or polychromatic light (Fig. 1). The absorbance *versus* concentration plots are shown as solid lines, and sensitivity (defined as absorbance/concentration according to ASTM [18] *versus* concentration plots are shown as broken lines. The sensitivity plots provide a good indication of changes in linearity. Note that the order of magnitude of the parameters b, c and ε in Eq. (3) does not influence the overall shape of the plots in Fig. 1. The range of the concentrations used for the calculations can be chosen so that they cover the whole range of absorbances of interest. The solid and broken lines labelled BL in Fig. 1 correspond to the absorbance and sensitivity plots, respectively, for the Beer's law case. The curves labelled 1%S and 10%S were calculated for monochromatic light at 1% and 10% stray light; percentage of stray light $= P_S/(P^0 + P_S)$. Although stray light is mostly anticipated as a linearity limiting factor at high absorbances, from the 1%S and 10%S curves it is obvious that stray light causes deterioration in linearity even at the lowest concentration and absorbance values.

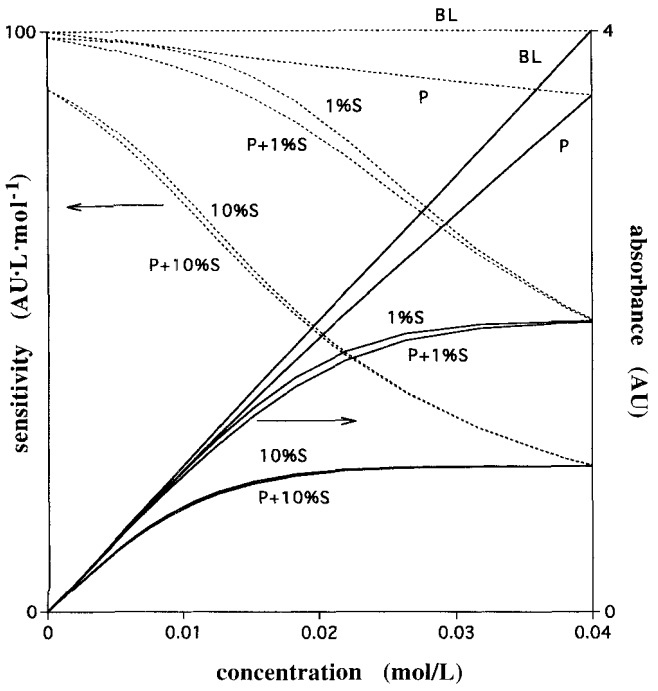

Figure 1. Absorbances calculated according to Eq. (3) (b = 0.01 cm, ε = 10000 L cm^{-1} mol^{-1} for BL) and corresponding sensitivities plotted as a function of concentrtation. See Section 2.2 for an explanation of labels.

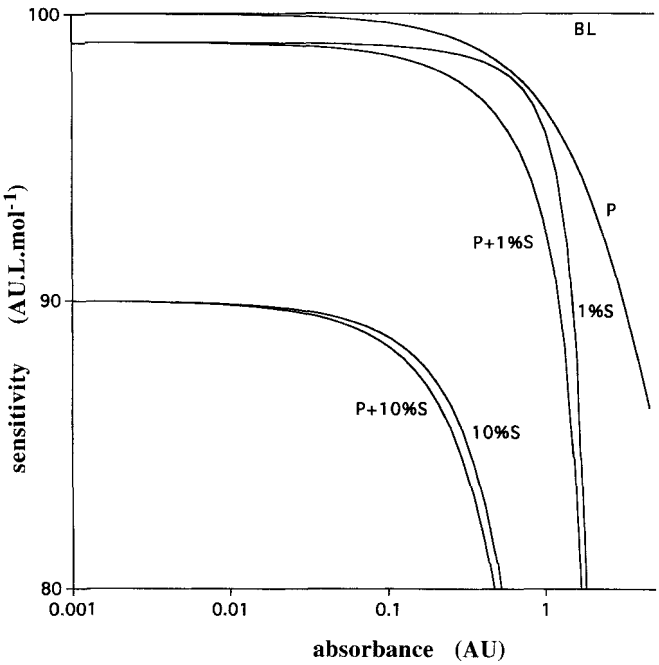

Figure 2. Calculated sensitivities plotted as a function of absorbance. See Section 2.2 for an explanation of labels.

The curve P was calculated for no stray light ($P_S = 0$) and for polychromatic light similar to a case that can be expected for an emission band lying on a slope of a broader absorption band: the molar absorptivities were chosen as ε = 3000, 6000, 10000, 14000, and 17000 (simulating the profile of an absorption band) and for light composed of five wavelengths having relative intensities of 1:4:8:4:1 (simulating the profile of an emission band). This corresponds to an emission-to-absorption bandwidth ratio (EBW/ABW) of approximately 0.3, which can be expected for most LEDs and typical solutes in the VIS region. Finally, the curves P+1%S and P+10%S incorporate the same polychromatic light as in the curve P but with additional 1% stray light or 10% stray light, respectively. It can be concluded from Fig. 1 that the deterioration of linearity as a result of polychromatic light is more ponounced at lower levels of stray light. This can be seen by comparison of the curves 10%S and P+10%S (which are almost superimposable) with the curves 1%S and P+1%S (which show significant differences). Consequently, it is possible for a polychromatic light source with a relatively low level of stray light (curve P+1%S) to exhibit better linearity than a monochromatic source with a high level of stray light (curve 10%S). Expressed quantitatively, a 1% decrease in sensitivity for polychromatic light without stray light (curve P) is reached at absorbance 0.31 AU, and for monochromatic light the same sensitivity decrease is caused by 2.1% stray light. Figure 1 allows the changes of detection linearity with concentration of the absorbing species to be judged. However, in most cases it is more practical to see sensitivity changes with the measured absorbance because such a graph then applies for any absorbing compound of any molar absorptivity. A plot of sensitivity *versus* absorbance is shown in Fig. 2, using the same labelling as for Fig. 1. The x-axis (absorbance) is logarithmic to enable the whole absorbance range to be shown and at the same time to reveal the important low-absorbance region in detail. This type of graph was used to plot the experimental data obtained in this study.

3 Materials and methods

3.1 Reagents

Water was treated with a Millipore (Bedford, MA, USA) Milli-Q water purification apparatus. All other reagents were of analytical grade. 2-(4,5-Dihydroxy-2,7-disulfo-3-naphthylazophenylarsenic acid (Arsenazo I, AI) was obtained from Aldrich (Milwaukee, WI, USA) and the zwitterionic Z1-Methyl (trimethylammoniumpropanesulfonate) was obtained from Waters (Milford, MA, USA). The background electrolyte (BGE) contained 0.50 mM AI, 0.20 M Z1-Methyl, 20 mM formic acid, and 50 mM diethanolamine, with the pH adjusted to 9.6. Before use the BGE was degassed by vacuum and filtered with a Millex-HA 0.45 μm disc filter (Millipore).

3.2 CE hardware

A Polymicro Technologies Inc. (Phoenix, AZ, USA) fused-silica capillary (60 cm length, 75–76 μm ID, length to detector: 52 cm) was used. The capillary was initially treated by washing with concentrated nitric acid (approximately 10 capillary volumes) and then with 1 M sodium hydroxide overnight. The instrument used was a Quanta 4000 (Waters) interfaced to a Maxima 820 data station (Waters). In addition to the original mercury lamp

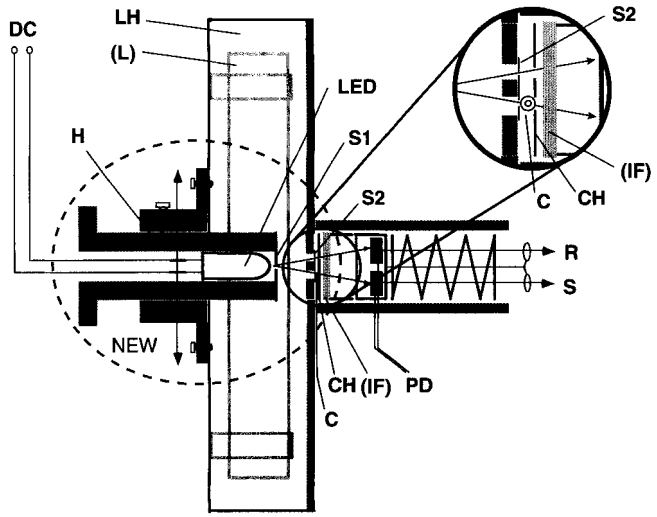

Figure 3. Schematic representation of the detector unit (not necessarily to scale). NEW, the part of the original detector unit where changes were made; LH, the original lamp holder; (L), position of the original Hg-lamp (before removal); LED, light-emitting diode; H, LED holder; DC, DC current supply; S1, slit approximately 1.5 mm; S2, razor blades serving for capillary self-adjustment and as a pair of 50 μm × 1 mm slits; C, capillary; CH, capillary holder (original); (IF), interference filter if used; PD, a pair of photodiodes; R, reference signal output; S, sample signal output. For other data see Section 3.2.

source (the line at 546.2 nm was used), two further light sources were constructed. The first was a 10W–12V tungsten halogen lamp (RS 568–506, RS Components Pty Ltd. Tullamarine, VIC, Australia) equipped with a 3 mm slit placed close to the bulb, and the bulb and slit were then mounted in the original Waters Hg-lamp holder in place of the Hg-lamp. The tungsten lamp source was used in combination with Waters 546 nm or 658 nm interference filters. The second alternative light source was constructed according to Fig. 3 using the original Waters Hg-lamp holder adapted to hold an LED with a 1.5 mm slit (S1, Fig. 3) attached to the LED. The surface of the polymer lens on the LED was made matt by lightly sanding the surface (the original round shape of the LED is retained) with P600 waterproof abrasive paper in order to achieve uniform spatial light intensity distribution in the frontal direction emerging from the slit. The light intensity distribution was monitored as a light image on a sheet of white paper placed a few cm in front of the LED. Both of the optional light sources were used with a home-made capillary self-alignment base using pairs of razor blades glued onto an aluminium base in a manner similar to that described previously [19]. As with the original light source supplied with the instrument, the slit width was approximately 50 μm and the slit length was 1 mm. The distance between the sample and reference slits was 3 mm (compared to 4 mm in the original source) because of the smaller geometric size of the LEDs compared to the mercury lamp.

3.3 CE separations

Injection was performed hydrostatically by elevating the sample at 100 mm for 20 s at the anodic side of the capillary. At the cathodic (detector) side a buffer reservoir of 4 mL volume was used. Instead of the standard 20 mL buffer reservoir at the anodic side, a plastic sample vial of approximately 0.6 mL was installed inside the standard 20 mL container. The run voltage was +25 kV.

3.4 On-capillary detector linearity

Potassium permanganate (0.08–200 mM solutions in 20 mM sodium periodate and 0.10 M phosphoric acid) and methylene blue (0.008–20 mM solutions in 40 mM cetyltrimethylammonium bromide (CTAB) in water-dimethylformamide 6/4 v/v) were used as absorbing probes to measure the on-capillary detector linearity as an absorbance-concentration relationship. Solutions with increasing concentration of the absorbing compound were sucked through the capillary by vacuum and then, after switching the vacuum off, the absorbance measurements were taken. The measured data were presented as sensitivity *versus* absorbance graphs, with sensitivity calculated for every data point according to ASTM [18] as absorbance of a solution of the absorbing probe divided by the concentration of the probe. The linearity range for each of the measured data sets was evaluated by performing exponential curve fits for the data in the interval from absorbance 0.001–0.2 AU. In this way it was ensured that data points for low absorbances (having more than 10% relative error) and data points from the most nonlinear parts of the curves at high absorbances were excluded from the fit. These curves were used to calculate the upper linear range absorbance for 95% and 90% sensitivity, *i.e.* for a drop in sensitivity of 5% or 10%, respectively (sensitivity was taken as 100% at an absorbance of 0.001). In order to calculate modelled absorbance-concentration plots, relative light intensities of the light sources were taken from their emission spectra at nine different wavelengths (the emission maximum plus four wavelengths on each side of the emission bandwidth in intervals of 5 nm) and given in arbitrary units. For the LED563B a sensitivity correction for the silicon photodiode detector was used, with the relative sensitivity taken as 0.33 at 400 nm with a linear increase to a relative sensitivity of 1.0 at 500 nm [7, 8, 20]. The relative light intensities were then used as the P_i^0 variable in Eq. (3). Finally, molar absorptivities of potassium permanganate and methylene blue were measured for all the wavelengths for which relative light intensities were determined and then used as ε_i in Eq. (3). Modelled sensitivity plots were then calculated: absorbances were calculated from Eq. (3) for the same range of concentrations as in the experiments and the parameters b and P_s were adjusted to obtain a good fit with the experimental data (the parameter b influences the fit mainly at low absorbandes/high sensitivity while the parameter P_s influences the fit mainly at high absorbances/low sensitivity).

3.5 Detector noise measurements

Detector noise was measured using 15 mM citrate–10 mM Tris buffer (pH 4.8) as BGE and a separation potential of 30 kV. After switching on the potential (no injection was performed) the signal was acquired with a frequency of 20 data points per second for a total interval of 2 min. As described earlier [21], using digital

Table 1. Specifications and performance characteristics for the LEDs used in this study

LED Designation	LED563A	LED563B	LED594	LED614	LED647	LED654
Manufacturer's specifications						
Catalog No.	RS 590–496	HLMP8509	RS 578-232	RS 578-200	HLMP8102	RS 564-015
Colour	Green	Green	Yellow	Orange	Red	Red
λ_{max} (nm)	563	568	590	620	637	660
Light output (mCd)	250	260	2500	1500	2000	3000
Maximum steady current (mA)	25	25	50	50	20	50
Measured characteristics						
λ_{max} (nm)	563	563	594	614	647	654
Band width (nm)	24	24	17	17	24	25

Table 2. Transmission characteristics of interference filters

Interference filter	IF546	IF658
Measured λ_{max} (nm)	546	659
$w_{(h/2)}$ (nm)	11.4	9.4

data on a selected linear piece of baseline, linear regression and then statistical analysis of the residuals were performed and finally the noise was determined as five times the calculated standard deviation of the data points at the selected baseline interval. In our series of experiments two 0.2 min long baseline segments (from 1.1 to 1.3 min and from 1.6 to 1.8 min) were evaluated and the average of the two baseline noise values was then calculated (the relative difference of the two values was less than 11% with all measurements).

3.6 LEDs and their emission spectra

LEDs (5 mm size, clear) were obtained from RS Components Pty Ltd. (VIC) and Farnell Electronic Components (Chester Hill, NSW, Australia). The LEDs were powered by a stabilised Good Will Laboratory Power Supply (Taiwan) using a resistor (180 Ω) connected in series, and the voltage was adjusted to read a current of 20 mA or 30 mA (voltage *ca.* 5.6 V or *ca.* 7.6 V, respectively). Emission spectra were measured using a Perkin-Elmer 650-10S fluorescence spectrophotometer, with the emission slit adjusted to 1 nm. The measured emission maximum wavelength λ_{max} and bandwidths at the emission band half height (EBW) together with the parameters specified by the manufacturer are given in Table 1.

3.7 Spectrophotometry

Spectrophotometric measurements were performed using a Cary 5 UV-VIS-NIR spectrophotometer using a slit width of 1 nm. The molar absorptivities of potassium permanganate and methylene blue were determined by measuring absorptions of standard solutions in 10 mm glass cells. The absorbance-concentration linearity of these solutions was determined in 2 mm (exactly 1.85 ± 0.01 mm) glass cells at 546 nm or 660 nm, respectively. Transmission characteristics of interference filters for 546 nm (IF546, Waters part No. 250459) and 568 nm (IF568, Waters LC 440 detector replacement part) were measured after placing the filter perpendicularly to the beam and positioning so that the whole beam was passing through the filter. Values for transmission maxima and peak width at half height are given in Table 2.

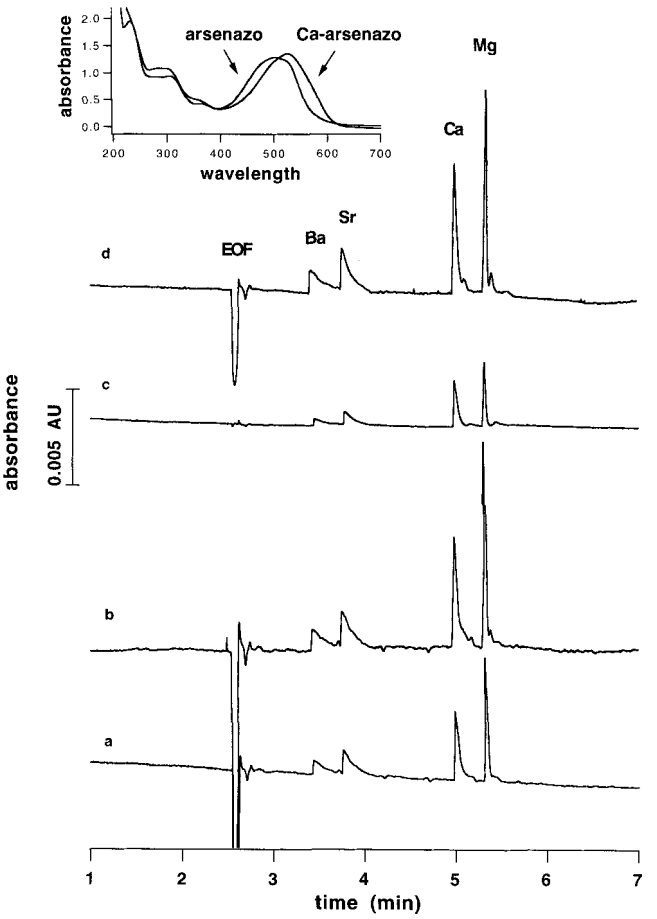

Figure 4. Electropherogram of Mg, Ca, Sr and Ba as Arsenazo I complexes. Detector: (a) Mercury lamp used with IF546 filter, (b) tungsten lamp used with IF546 filter, (c) LED590, (d) LED568. The absorption spectra for arsenazo I and its Ca-complex are shown in the inset. These spectra were obtained for ligand and metal concentrations of 0.1 mM in acetate-ammonia buffer pH 9.5 and 10 mm cell. For other conditions, see Section 3.3.

4 Results and discussion

4.1 Noise

The most common LEDs cover the approximate wavelength range of 560–660 nm. This range is particularly relevant to the detection of metal complexes of metallochromic dyes and this application has been used to evaluate the performance of LED-based detectors. Any practical applicability of LEDs as light sources for

Table 3. Baseline noise (five times the standard deviation) for various detector set-ups[a)]

Detector	Hg lamp	Tungsten lamp + IF546	LED 563A	LED 563B	LED 594	LED 614	LED 647	LED 654	Tungsten lamp + IF658
Noise ($\times 10^{-5}$ AU)	6.5	13.9	6.7	6.3	5.2	5.1	3.8	3.0	13.9

a) Detector time constant 0.1 s, data acquisition frequency 20 Hz

absorption detection depends on the observed noise levels. In Fig. 4, electropherograms of a separation of Ba, Sr, Ca and Mg as arsenazo I complexes are presented, with different light sources being used for detection. All four electropherograms show a similar detection response and the LED-based detectors exhibit lower noise compared to tungsten and mercury lamps. However, the BGE used in this case has a significant absorbance due to the added arsenazo I and consequently the level of noise is dependent on the wavelength of the light source. In order to avoid any noise caused by changes in an absorbing background, the noise measurements were carried out in a nonabsorbing BGE, but still under real electrophoretic conditions. The results (see Table 3) show that in the detector set-up used for these measurements the LEDs exhibited up to five times lower noise than the mercury and tungsten lamps. The lowest noise level obtained was 3×10^{-5} AU (LED654) for a detector time constant of 0.1 s, corresponding to *ca.* 1×10^{-5} AU for a rise time or integration time of 1 s. This is in a good agreement with literature data: as pointed out by Dasgupta *et al.* [1], the intensity stability of LEDs should allow absorbance noise values of *ca.* 1×10^{-5} and similar values have been reported for several LED-based absorption detectors [1, 2].

The different light intensities of the LEDs is probably the main reason for their different noise levels, with the LED654 offering the highest light output of all the LEDs (Table 1) and also the lowest noise. However, when comparing the noise levels for LEDs with those of the mercury and tungsten lamp based detectors, the differences in performance cannot be explained only by variations in light intensity. For example, the light intensities at the detector for LED563A and LED563B were roughly half of that for Hg546, but the observed noise levels were approximately the same. The noise is influenced by additional factors such as the stability of the source and the ruggedness of the optics [1].

4.2 Linearity measurements

For linearity investigations all light sources and absorption probes were spectrally characterised. Examples of the emission spectra of the LEDs are in Fig. 5, from which it is clear that the LEDs are more polychromatic sources compared to interference filters. In the case of potassium permanganate as an absorbing probe, periodate was added to stabilise the solution [22], and to ensure the absence of any chemical nonlinearity effects the absorbance-concentration dependence was measured using 2 mm cells and a high quality spectrophotometer. Since methylene blue is well known to sorb onto fused silica capillary walls from aqueous solutions [23], dimethylformamide was added to the solution and excess CTAB was added (40 mM) to compete for the silanol

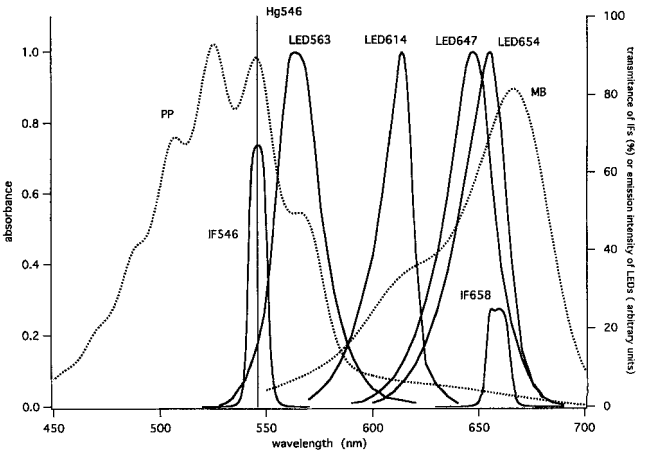

Figure 5. Emission spectra of LEDs and absorption spectra of interference filters and test compounds. IF, interference filter of specified wavelength; Hg 546, mercury lamp at 546 nm; LED, light-emitting diode of the specified wavelength; PP, potassium permanganate; MB, methylene blue.

adsorption sites and also to provide sufficient interactions of the solute with the charged CTAB molecules to prevent any changes in molar absorptivity with increasing methylene blue concentration [4]. Again, absorbance-concentration linearity of the methylene blue solutions was checked using spectrophotometry in 2 mm cells.

The observed linearity data are plotted as discrete data points in Figs. 6 and 7 for permanganate and methylene blue as probes, respectively. Note that plotting sensitivity *versus* absorbance instead of concentration makes both figures directly comparable even though the molar absorptivities of the test substances are very different. The linearity of the experimental data was evaluated by calculating the upper linear range absorbance for 95% and 90% sensitivity, *i.e.* for a drop in sensitivity caused by nonlinearity of 5% or 10%, respectively. The results are given in Table 4 and show that although the mercury lamp (Hg546) is an almost ideal monochromatic light source, its linearity is the worst of the light sources tested. In addition, the tungsten lamp with the IF658 filter exhibited poorer linearity than LED654 and LED648, despite its narrower spectral bandwidth. These observations cannot be explained without consideration of the level of stray light for each detector set-up.

The stray light level can be determined together with the effective path length by fitting the theoretical model according to Eq. (3) to the experimental linearity data. Using the values of relative light intensities and molar absorptivities at given wavelengths, modelled curves (broken and solid lines in Figs. 6 and 7) were calculated using Eq. (3), with the path lengths and stray light values

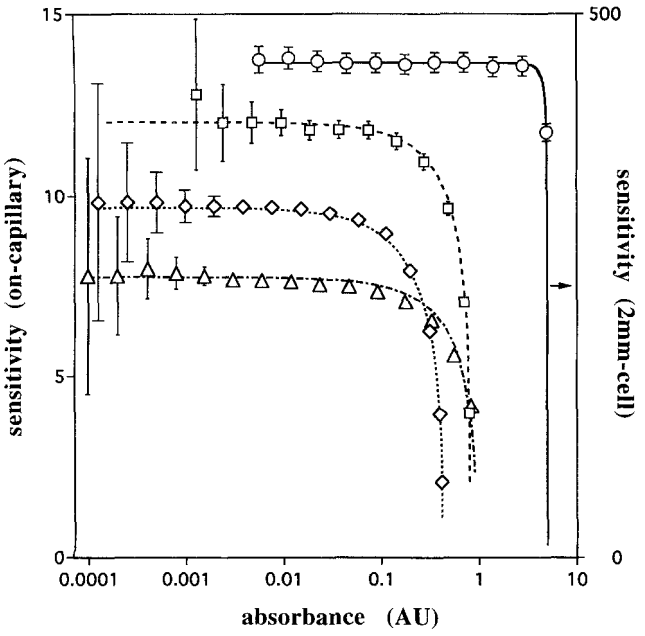

Figure 6. Experimental sensitivity *versus* absorbance data for potassium permanganate, together with curves fitted from Eq. (4). Detector: (○) Cary 5 spectrophotometer, (◇) Hg lamp at 546 nm, (□) tungsten lamp with IF546 filter, (△) LED563. For other conditions, see Section 3.4.

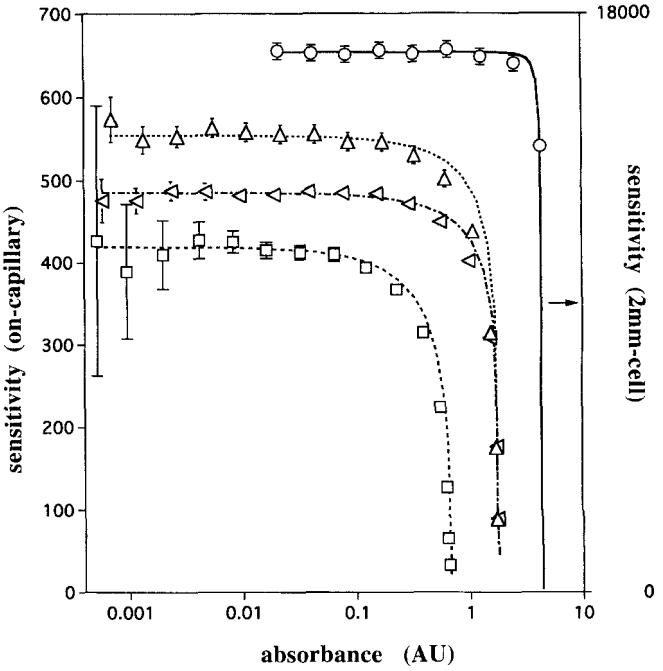

Figure 7. Experimental sensitivity *versus* absorbance data points for methylene blue, together with curves fitted from Eq. [4]. Detector: (○) Cary 5 spectrophotometer; (△) LED654; (□) tungsten lamp with IF658 filter; (◁) LED648. For other conditions, see Section 3.4.

Table 4. Upper linear range absorbance (A_{max}) for 95% and 90% sensitivity and optical parameters of the various detection set-ups

Detector	A_{max} (sens. = 100% at 0.001 AU)		Parameters determined through modelling	
	95%	90%	Stray light %	Effective path length mm
Hg546	0.07	0.14	38	0.064
W+IF546	0.16	0.32	18	0.061
LED563	0.10	0.21	11	0.065
Cary 5, 546 nm	4.6	4.8	0.0011	1.86
LED647	0.51	0.76	1.6	0.076
LED654	0.49	0.74	1.7	0.076
LED654+IF658	0.59	0.88	2.2	0.070
W+IF658	0.10	0.18	22	0.064
Cary 5, 658 nm	4.0	4.2	0.0041	1.86

being chosen to give the best fit to the experimental data (see Table 4). The agreement of the modelled curves with the experimental data shows that this is a simple method to determine both the stray light percentage and effective path length, in comparison to the commonly used method of measurement of transmittance for a totally absorbing solution [6, 9, 10] which results only in determination of the level of stray light. Furthermore, disagreement between experimental data and the corresponding modelled curve would indicate the influence of an additional process not included in the model. The fact that agreement in the case of LED563 is not as good as in the other cases may be caused by the necessity to approximate the LED563 emission spectrum by several (nine) values of relative emission intensities P_i and corresponding permanganate molar absorptivities ε_i. Data for LED654 used with the IF658 filter are not plotted since the results were similar to those for the LED654 alone.

The level of stray light in each detector set-up can now be used to explain most of the observed differences in linearity. In agreement with theory, the results (Table 4) show the stray light as the main factor which determines linearity under the typical conditions in on-capillary detection in CE. The mercury line source (Hg546) used in an optical set-up giving a high level of stray light exhibited linearity which was poorer than all of the tested LEDs which were used in set-ups providing lower levels of stray light. The difference of the stray light level between the mercury lamp detector and all the others may be partly caused by the fact that the mercury lamp detector had to be used with different self-alignment bases and slits than the other sources (see Section 3.2). The influence of the polychromaticity of the light source on linearity is small under the conditions used, but can be expected to be more significant at lower levels of stray light (*ca.* below 2%), for broad emission band LEDs (band half width above 25 nm), or for analytes

with narrow absorption bands (band half width below 50 nm). The path lengths determined from Fig. 6 and 7 are shown in Table 4; note that the calculated value of 1.86 mm for the spectrophotometer is in good agreement with the actual cell width of 1.85 mm, and the calculated effective path lengths of 61–76 μm for the capillary are quite reasonable for a capillary ID of 75 μm and slit width of 50 μm. Using the equation for effective path length derived by Bruin *et al.* [12], there is a 69 μm effective path length for a 75 μm ID capillary and 50 μm slit (for parallel light beams and no focusing effect of the capillary).

Knowledge of the effective path length is useful for two reasons. First, a considerably shorter effective path length than the actual capillary internal diameter indicates that a broad cross-section of the capillary is illuminated, which may cause higher levels of stray light (this trend is evident in Table 4). Second, the shorter the effective path length, the greater the variety of actual path lengths in the detector and hence the greater contribution to nonlinearity in the same way as caused by polychromatic light [6, 9]. Use of a slit width approaching the capillary inner diameter would result in considerable path length variability and consequently in absorbance nonlinearity, necessitating inclusion of an additional factor in the mathematical model in a similar way as Bruin *et al.* [13].

5 Concluding remarks

For on-capillary detection in CE, LEDs have been demonstrated to be a good alternative to other light sources in the range of ca. 560 to 660 nm. At the levels of stray light typical for the cross-beam on-capillary detection in CE (2–20%) the stray light is the main factor which limits linearity, even in the low-absorbance range. Under these conditions the linearity decrease introduced by the polychromaticity of a typical LED is likely to be negligible for most solutes. At lower levels of stray light (below 2%) the influence on linearity of the polychromaticity of the light source has to be considered. Modelling of absorbance *versus* concentration and sensitivity *versus* absorbance dependencies and fitting them to measured data is a relatively simple way to determine effective path length and the percentage of stray light as the basic parameters of an optical set up. Under the conditions used, the observed baseline noise of an LED-based detector was found to be markedly better than for mercury or tungsten lamps.

Financial support for this work from Waters Corporation is gratefully acknowledged.

Received June 24, 1996

6 References

[1] Dasgupta, P. K., Bellamy, H. S., Liu, H., Lopez, J. L., Loree, E. L., Morris, K., Petersen, K., Mir, K. A., *Talanta* 1993, *40*, 53–74.
[2] Bruno, A. E., Maystre, F., Krattiger, B., Nussbaum, P., Gassmann, E., *Trends Anal. Chem.* 1994, *13*, 190–198.
[3] Tong, W., Yeung, E. S., *J. Chromatogr.* 1995, *718*, 177–185.
[4] *Encyclopedia of Lasers and Optical Technology*, Academic Press, San Diego 1991, p. 423.
[5] Skoog, D. A., Leary, J. J., *Principles of Instrumental Analysis*, Harcourt Brace College Publishers, Orlando 1992, Chapter 7, pp. 123–131.
[6] Ingle, J. D., Crouch, S. R., *Spectrochemical Analysis*, Prentice Hall, Englewood Cliffs 1988, p. 374–380.
[7] Hauser, P. C., Chiang, D. W. L., *Talanta* 1993, *40*, 1193–1200.
[8] Hauser, P. C., Rupasinghe, T. W. T., Cates, N. E., *Talanta* 1995, *42*, 605–612.
[9] Walbroehl, Y., Jorgenson, J. W., *J. Chromatogr.* 1984, *315*, 135–143.
[10] Sepaniak, M. J., Swaile, D. F., Powell, A. C., *J. Chromatogr.* 1989, *480*, 185–196.
[11] Wang, T., Hartwick, R. A., *J. Chromatogr.* 1989, *462*, 147–154.
[12] Bruno, A. E., Gassmann, E., Periclè, N., Anton, K., *Anal. Chem.* 1989, *61*, 876–883.
[13] Bruin, G. J. M., Stegeman, G., van Asten, A. C., Xu, X., Kraak, J. C., Poppe, H., *J. Chromatogr.* 1991, *559*, 163–181.
[14] *Standard Practice for Testing Fixed-Wavelength Photometric Detectors Used in Liquid Chromatography*, ANSI/ASTM E685–79, American Society for Testing and Materials, Philadelphia, PA 1979.
[15] Cassidy, R., Janoski, M., *LC.GC* 1992, *10*, 692–696.
[16] Fawlis, L. A., Scott, R. P., *J. Chromatogr.* 1963, *11*, 1–10.
[17] Dorschel, C. A., Ekmanis, J. L., Oberholtzer, J. E., Warren Jr., R. V., Bidlingmeyer, B. A., *Anal. Chem.* 1989, *61*, 951A–968A.
[18] *Annual Book of ASTM Standards*, American Society for Testing and Materials, Philadelphia 1988, 14.01, pp. 149–158.
[19] Fanali, S., Ossicini, L., Foret, F., Boček, P., *J. Microcolumn Sep.* 1989, *1*, 190–194.
[20] Wilson, J., Hawkes, J. F. B., *Optoelectronics*, Prentice Hall, New York 1986.
[21] Macka, M., Seménková, L., Borák, J., Mikes, V., Popl, M., *J. Liq. Chromatogr.* 1993, *16*, 2359–2386.
[22] *Tables of spectrophotometric absorption data of compounds used for the colorimetric determination of elements*, Butterworths, London 1963, p. 337.
[23] Williams, S. J., Bergström, E. T., Goodall, D. M., Kawazumi, H., Evans, K. P., *J. Chromatogr.* 1993, *636*, 39–45.